Separation of Energy Scales in Undoped $YbRh_2Si_2$ Under Hydrostatic Pressure

Yoshi TOKIWA*, Philipp GEGENWART, Christoph GEIBEL[1], and Frank STEGLICH[1]

I. Physikalisches Institut, Georg-August-Universität Göttingen, D-37077 Göttingen, Germany
[1]*Max-Planck-Institute for Chemical Physics of Solids, D-01187 Dresden, Germany*

The temperature–magnetic field (T–H) phase diagram of $YbRh_2Si_2$ in the vicinity of its quantum critical point is investigated by low-T magnetization measurements. Our analysis reveals that the energy scale $T^\star(H)$, previously related to the Kondo breakdown and terminating at 0.06 T for $T \to 0$, remains unchanged under pressure, whereas the antiferromagnetic critical field increases from 0.06 T ($P = 0$) to 0.29 T ($P = 1.28$ GPa), resulting in a crossing of $T_N(H)$ and $T^\star(H)$. Our results are very similar to those on $Yb(Rh_{1-x}Co_x)_2Si_2$, proving that the Co-induced disorder can not be the reason for the detachment of both scales under chemical pressure.

Heavy fermion (HF) metals, i.e., periodic lattices of certain f-elements, are ideally suited to study the interplay of competing interactions (Kondo- vs RKKY-interaction), which can lead to a continuous phase transition at zero-temperature, driven by pressure, doping or magnetic field.[1)] In the approach of the quantum critical point (QCP) the magnetic order parameter fluctuations grow continuously in spatial and temporal dimensions, causing strong deviations from Landau's Fermi liquid (LFL) theory. Such non-Fermi liquid (NFL) states are characterized by a single-excitation energy scale, which vanishes at the QCP.[2–4)] This results, e.g., in a divergence of the Grüneisen ratio, $\Gamma \propto \beta/C$, or magnetic Grüneisen parameter $\Gamma_{mag} \propto (-dM/dT)/C$, ($\beta$: volume thermal expansion, C: electronic specific heat, M: magnetization) for QCPs tuned by pressure and magnetic field, respectively.[5)] Experiments on the HF metals $CeCu_{6-x}M_x$ (M = Au,[6)] Ag[7)]) and $YbRh_2Si_2$[8–10)] are incompatible with the standard picture of an antiferromagnetic (AF) QCP, which describes a spin-density-wave transition. Unconventional quantum criticality,[11–14)] which qualitatively differs from the predictions of the standard theory, may arise due to a destruction of Kondo screening, leading to a decomposition of the heavy quasiparticles into conduction electrons and local magnetic moments.

In this letter, we focus on the clean stoichiometric HF metal $YbRh_2Si_2$, located very close to a QCP.[15)] Because of the very weak AF order below $T_N = 0.07$ K, a tiny variation of an external control parameter is sufficient to tune the system through the QCP. The AF order may be suppressed either by small amounts of Ge-, La-, or Ir-doping[8,16,17)] or magnetic fields of $H_N \approx 0.06$ T and ≈ 0.7 T, applied perpendicular and parallel to the tetragonal c-axis, respectively.[18)] At $H > H_N$, heavy LFL behavior is found in the low-T electronic specific heat, magnetic susceptibility and electrical resistivity, with diverging coefficients in the approach of the critical field.[19)] Correspondingly, a stronger than logarithmic divergence of $C(T)/T$ and linear T-dependence of the electrical resistivity has been found in the quantum critical regime.[8)] These NFL effects, together with the Grüneisen ratio divergences[20,21)] could not be described within the itinerant theory for an AF QCP. Furthermore, evidence for strong ferromagnetic (FM) fluctuations, competing with the AF ones near the QCP have been found in bulk suscpetibility[19)] and nuclear magnetic-resonance experiments.[22)] A quantum tricritical-point scenario has been proposed to account for these observations.[23)] However, this model predicts a saturation of the specific heat coefficient in the approach of the QCP, as in the standard theory,[4)] in contrast to the specific heat results. The absence of a metamagnetic signature in the magnetization at the field-tuned QCP[18)] seems also incompatible with a field-driven critical valence transition.[24)] Alternatively, the quasiparticle mass divergence may hint at a destruction of the Kondo effect.[8)] Indeed, a drastic change of the Hall coefficient upon tuning through a line $T^\star(H)$ which vanishes at $H = H_N$ at the QCP has been found, suggesting a strong change of the Fermi volume due to the localization of the 4f-electrons at the QCP.[9)] Thermodynamic and transport measurements such as magnetization, magnetostriction, magnetoresistance all revealed related crossovers whose full widths at half maxima (FWHM) vanish in the $T \to 0$ limit.[10)] Further thermodynamic evidence for the existence of this additional energy scale arises from maxima in the field dependence of $-\Delta M/\Delta T \approx -dS/dH$, indicating a characteristic reduction of spin entropy upon crossing $H^\star$, i.e., the field corresponding to $T^\star(H)$, at constant temperature.[21)]

To study the interplay of the Kondo-breakdown with the AF QCP in $YbRh_2Si_2$, slightly doped single crystals in which Rh has been partially substituted by isoelectronic but either smaller Co or larger Ir have recently been investigated at low temperatures.[17)] Most remarkably, the scale $T^\star(H)$ remains virtually unchanged when the boundary of the AF ground state $T_N(H)$ is either enlarged or suppressed in the former and latter case, respectively. For $Yb(Rh_{1-x}Ir_x)_2Si_2$, a novel spin-liquid type ground state emerges, in which the f-moments are neither Kondo-screened nor ordered, whereas for $Yb(Rh_{1-x}Co_x)_2Si_2$ the field-tuned QCP at H_N may be of itinerant nature, since it is located within the large Fermi-

*E-mail: ytokiwa@gwdg.de

surface regime at $T < T^\star(H)$.[17] Since disorder may strongly influence quantum criticality in HF systems, we have performed hydrostatic pressure experiments on clean undoped $YbRh_2Si_2$ and compare the results with ambient-pressure ones on $Yb(Rh_{1-x}Co_x)_2Si_2$.

High-quality single crystals ($\rho_0 = 1\,\mu\Omega\,cm$) were grown from In-flux as described earlier.[15] The DC magnetization was measured utilizing a high-resolution capacitive Faraday magnetometer.[25] In order to determine the magnetization under hydrostatic pressure, a miniaturized CuBe piston-cylinder pressure cell of 6 mm outer diameter and 3.2 g total weight has been designed. The piston is made from NiCrAl, a hard material with a relatively small magnetization. The magnetization of the pressure cell including the 6.0 mg $YbRh_2Si_2$ single crystal mounted on the magnetometer, can be detected with a resolution as high as 10^{-5} emu. The contribution of the sample to the total magnetization of the sample and pressure cell is larger than 63% in the entire field and temperature range. The pressure is determined by the difference between the superconducting transitions of two small Sn samples; one placed inside the pressure-transmitting medium (Daphne oil) together with the $YbRh_2Si_2$ sample, the other one outside the pressure cell. The T_c values are determined using a commercial SQUID magnetometer. Magnetization data up to 11.5 T to study the suppression of HF behavior at high fields under pressure have been published before.[26] Here, we concentrate on the low-field range close to the AF QCP.

Figure 1 shows the magnetization for $H \perp c$ at 0, 0.64 and 1.28 GPa at various temperatures. For each temperature, the magnetization at any field increases significantly under pressure. The AF critical fields H_N indicated by arrows are shifted from 0.06 to 0.14 and 0.29 T at 0.64 and 1.28 GPa, respectively. At 1.28 GPa, $M(H)$ shows an additional anomaly at 0.08 T, at a second AF transition, which has also been observed in $Yb(Rh_{0.93}Co_{0.07})_2Si_2$.[17] In $M(H)$, the signature of $H^\star$ is a change in slope from higher to lower values below and above $H^\star$, giving rise to a convex shape of the magnetization curve which broadens with increasing temperature.[10] Similar behavior is found under hydrostatic pressure: As shown in the inset in Fig. 1(a), the $M(H)$ traces at different pressure, scaled by the magnetization values at 1 T are almost identical at similar temperatures. Previously, $\widetilde{M}(H) = M + \chi H$ rather than $M(H)$ has been analyzed for $YbRh_2Si_2$ at ambient pressure[10] as well as for $Yb(Rh_{0.93}Co_{0.07})_2Si_2$.[17] Here $\chi = dM/dH$ denotes the differential susceptibility and $\widetilde{M} = d(MH)/dH$ is proportional to the field-derivative of the magnetic free energy contribution $-MH$.[10]

Representative $\widetilde{M}(H)$ data at 0.54 K (0.50 K only for $P = 0$) at different pressures are shown in Fig. 2. We used the field integral of the same empirical function of the form $f(H,T) = A_2 - (A_2 - A_1)/[1 + (H/H_0)^p]$ as used in refs. 10, 17 to describe the data with the parameters given in Table I. We note, that the obtained position of H_0 remains almost unchanged under pressure. At temperatures below T_N, the anomaly due to AF order interferes with the broad kink which marks $T^\star$. Under a pressure of 0.64 GPa, $\widetilde{M}(H)$ at 0.1 K exhibits a peak at H_N, which shifts to lower field as temperature is increased up to T_N, following the AF phase boundary (see inset). This peak due to AF order disappears at higher temperatures where only the broad kink remains. This kink indicates the cross-over field H_0 and its position shifts to higher fields as temperature is increased. Remarkably, both H_0 and the full width at half maximum (FWMH)

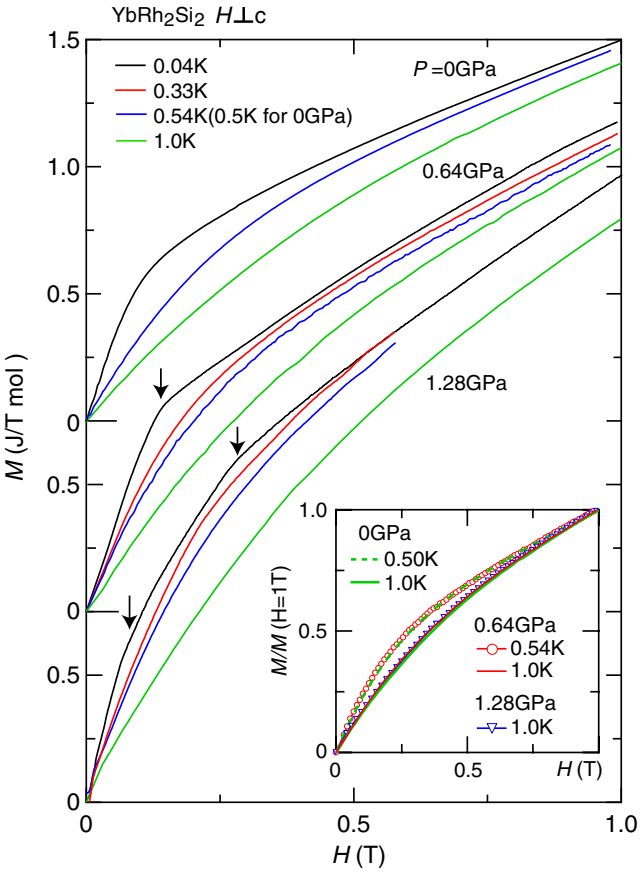

Fig. 1. (Color online) Magnetization curves of $YbRh_2Si_2$ in a field perpendicular to c-axis at pressures 0, 0.64 and 1.28 GPa for different temperatures. Curves for 0 and 0.64 GPa are shifted vertically for clarity. Arrows indicate AF phase transitions. Inset: magnetization, normalized by its value at 1 T, vs field.

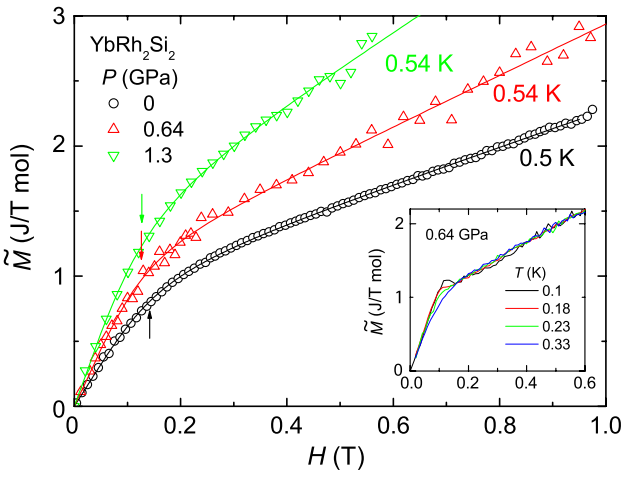

Fig. 2. (Color online) $\widetilde{M}(H) = M + \chi H$ of $YbRh_2Si_2$ at ambient pressure, as well as 0.64 and 1.28 GPa for 0.5, 0.54, and 0.54 K, respectively. The lines are fits with an empirical crossover function using the parameters given in Table I. Arrows indicate the crossover field H_0. Inset: $M + \chi H$ under a pressure of 0.64 GPa at different temperatures.

Table I. Parameters for the description of $\tilde{M}(H)$ shown in Fig. 2 and the respective ones for $Yb(Rh_{0.93}Co_{0.07})_2Si_2$ by the empirical crossover function $\int f dH$ with $f(H,T) = A_2 - (A_2 - A_1)/[1 + (H/H_0)^p]$.[9] Here A_1 and A_2 represent the slopes of $\tilde{M}(H)$ below and above the crossover, respectively. H_0 is the crossover field and the exponent p is a measure for the broadening of the crossover.

P (GPa)	T (K)	H_0 (T)	p	FWHM (T)
0	0.5	0.14 ± 0.015	3.1 ± 0.15	0.14 ± 0.04
0.64	0.54	0.12 ± 0.015	3.4 ± 0.7	0.12 ± 0.03
1.28	0.54	0.12 ± 0.015	2.8 ± 0.7	0.125 ± 0.04
Co-7%[17]	0.5	0.125 ± 0.015	2.3 ± 0.3	0.13 ± 0.04

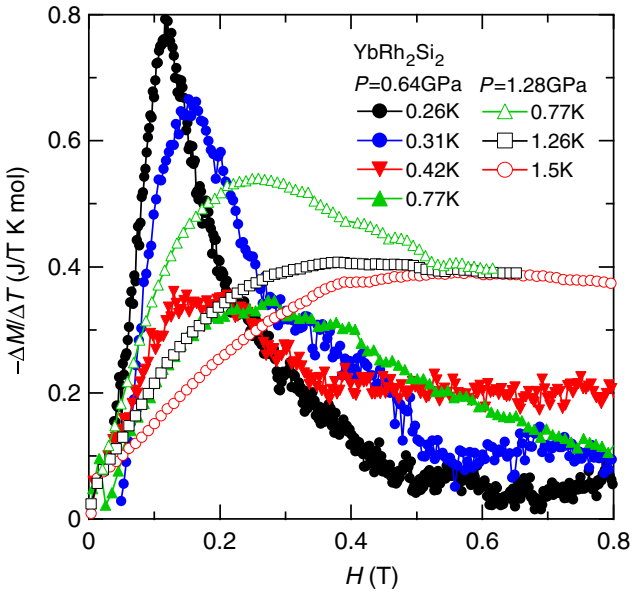

Fig. 3. (Color online) Magnetization difference divided by temperature increment, $-\Delta M/\Delta T$, vs magnetic field for $YbRh_2Si_2$ under hydrostatic pressures of 0.64 and 1.28 GPa, obtained from isothermal magnetization measurements at different temperatures (see text).

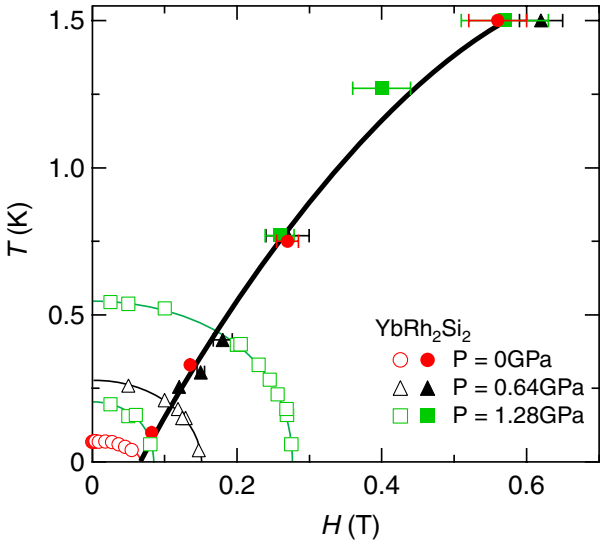

Fig. 4. (Color online) H–T phase diagram of $YbRh_2Si_2$ at hydrostatic pressures of 0, 0.64 and 1.28 GPa. Open and filled symbols represent the AF transition and maxima in $-\Delta M/\Delta T$, respectively. Solid lines are guides to the eye.

determined at the various pressures are almost identical. Also, they nicely agree with the values obtained for $Yb(Rh_{0.93}Co_{0.07})_2Si_2$.[17]

We obtained the magnetization difference divided by temperature increment, $-\Delta M/\Delta T = -[M(T + \Delta T, H) - M(T - \Delta T, H)]/2\Delta T$, from isothermal magnetization data at various different temperatures under hydrostatic pressure. As discussed previously,[21] $\Delta M/\Delta T$ probes the field derivative of the entropy through the Maxwell relation, $\Delta M/\Delta T \approx dM/dT = dS/dH$. In Fig. 3, we show $-\Delta M/\Delta T$ at temperatures above T_N, i.e., outside the AF phase, since the anomaly due to the AF ordering formation interferes with the signature of $H^\star$. At ambient pressure, $-\Delta M/\Delta T$ exhibits a maximum very close to $H^\star$ (ref. 21). Similar maxima, which broaden and shift to higher fields upon increasing temperature, are also found under hydrostatic pressure. The positions of the maxima, plotted in Fig. 4, indicate inflection points in the field dependence of the entropy, which, as found previously[21] are related to $H^\star$.

As shown in the phase diagram of Fig. 4, the AF phase boundary is expanded with hydrostatic pressure, and at $P = 1.28$ GPa there are two AF phases at T_N and T_L.[27] On the other hand, $T^\star$ is independent of pressure, resulting in a crossing of $T^\star(H)$ and $T_N(H)$ and different critical fields where the two temperature scales vanish. This is very similar to what has been observed for chemically pressurized $Yb(Rh_{1-x}Co_x)_2Si_2$.[17] Therefore, the disorder introduced by partial Co substitution of Rh atoms in the latter series, which enhances the residual resistivity from 1 μΩ cm at $x = 0$ to 10.7 μΩ cm at $x = 0.07$, does not influence the low-T phase diagram and can not be responsible for the detachment of the two energy scales. Future pressure experiments should focus on the nature of the AF QCP. Since under pressure $H_N > H^\star$ it is presumably of standard SDW type. We also note, that volume expanded $Yb(Rh_{0.94}Ir_{0.06})_2Si_2$, with a residual resistivity of $\rho_0 = 14$ μΩ cm, has been studied by electrical resistivity.[28] Translating the chemically-induced volume expansion to a pressure of $\Delta p = -0.06$ GPa has revealed the identical temperature versus pressure phase diagram (at $H = 0$) as found in undoped $YbRh_2Si_2$,[27] proving that disorder introduced by substitution has only minor effects.

In conclusion, we have measured the magnetization of $YbRh_2Si_2$ under hydrostatic pressure in order to investigate the boundary of the AF phase as well as the location of the crossover line $T^\star(H)$. While the former is increasing with pressure, the latter remains unchanged, resulting in an intersection between $T^\star(H)$ and $T_N(H)$. The entropic signature of $T^\star(H)$ found at ambient pressure[21] is confirmed. Our results indicate, that the separation of the AF from the Kondo breakdown QCP in doped $YbRh_2Si_2$[17] cannot be due to disorder but is clearly related to the change of the unit-cell volume.

Acknowledgments

We would like to thank R. Borth and C. Klausnitzer for technical support and M. Brando, J. Ferstl, S. Friedemann, C. Krellner, T. Nakanishi, M. Nicklas, Q. Si, G. Sparn, and T. Westerkamp for useful discussions. This work was supported by the DFG research unit 960 “Quantum phase transitions”.

1) P. Gegenwart, Q. Si, and F. Steglich: Nat. Phys. **4** (2008) 186.
2) J. A. Hertz: Phys. Rev. B **14** (1976) 1165.
3) A. J. Millis: Phys. Rev. B **48** (1993) 7183.
4) T. Moriya and T. Takimoto: J. Phys. Soc. Jpn. **64** (1995) 960.
5) L. Zhu, M. Garst, A. Rosch, and Q. Si: Phys. Rev. Lett. **91** (2003) 066404.
6) A. Schröder, G. Aeppli, R. Coldea, M. Adams, O. Stockert, H. v. Löhneysen, E. Bucher, R. Ramazashvili, and P. Coleman: Nature **407** (2000) 351.
7) R. Küchler, P. Gegenwart, K. Heuser, E.-W. Scheidt, G. R. Stewart, and F. Steglich: Phys. Rev. Lett. **93** (2004) 096402.
8) J. Custers, P. Gegenwart, H. Wilhelm, K. Neumaier, Y. Tokiwa, O. Trovarelli, C. Geibel, F. Steglich, C. Pepin, and P. Coleman: Nature **424** (2003) 524.
9) S. Paschen, T. Lühmann, S. Wirth, P. Gegenwart, O. Trovarelli, C. Geibel, F. Steglich, P. Coleman, and Q. Si: Nature **432** (2004) 881.
10) P. Gegenwart, T. Westerkamp, C. Krellner, Y. Tokiwa, S. Paschen, C. Geibel, F. Steglich, E. Abrahams, and Q. Si: Science **315** (2007) 969.
11) Q. Si, M. S. Rabello, K. Ingersent, and J. L. Smith: Nature **413** (2001) 804.
12) P. Coleman, C. Pépin, Q. Si, and R. Ramazashvili: J. Phys.: Condens. Matter **13** (2001) R723.
13) T. Senthil, M. Voijta, and S. Sachdev: Phys. Rev. B **69** (2004) 035111.
14) I. Paul, C. Pèpin, and M. R. Norman: Phys. Rev. Lett. **98** (2007) 026402; C. Pèpin: Phys. Rev. Lett. **98** (2007) 206401.
15) O. Trovarelli, C. Geibel, S. Mederle, C. Langhammer, F. M. Grosche, P. Gegenwart, M. Lang, G. Sparn, and F. Steglich: Phys. Rev. Lett. **85** (2000) 626.
16) J. Ferstl, C. Geibel, F. Weickert, P. Gegenwart, T. Radu, T. Lühmann, and F. Steglich: Physica B **359–361** (2005) 26.
17) S. Friedemann, T. Westerkamp, M. Brando, N. Öeschler, S. Wirth, P. Gegenwart, C. Krellner, C. Geibel, and F. Steglich: Nat. Phys. **5** (2009) 465.
18) P. Gegenwart, Custers J, C. Geibel, K. Neumaier, T. Tayama, K. Tenya, O. Trovarelli, and F. Steglich: Phys. Rev. Lett. **89** (2002) 056402.
19) P. Gegenwart, J. Custers, Y. Tokiwa, C. Geibel, and F. Steglich: Phys. Rev. Lett. **94** (2005) 076402.
20) R. Küchler, N. Oeschler, P. Gegenwart, T. Cichorek, K. Neumaier, O. Tegus, C. Geibel, J. A. Mydosh, F. Steglich, L. Zhu, and Q. Si: Phys. Rev. Lett. **91** (2003) 066405.
21) Y. Tokiwa, T. Radu, C. Geibel, F. Steglich, and P. Gegenwart: Phys. Rev. Lett. **102** (2009) 066401.
22) K. Ishida, K. Okamoto, Y. Kawasaki, Y. Kitaoka, O. Trovarelli, C. Geibel, and F. Steglich: Phys. Rev. Lett. **89** (2002) 107202.
23) T. Misawa, Y. Yamaji, and M. Imada: J. Phys. Soc. Jpn. **77** (2008) 093712.
24) S. Watanabe, A. Tsuruta, K. Miyake, and J. Flouquet: J. Phys. Soc. Jpn. **78** (2009) 104706.
25) T. Sakakibara, H. Mitamura, T. Tayama, and H. Amitsuka: Jpn. J. Appl. Phys. **33** (1994) 5067.
26) Y. Tokiwa, P. Gegenwart, T. Radu, J. Ferstl, G. Sparn, C. Geibel, and F. Steglich: Phys. Rev. Lett. **94** (2005) 226402.
27) S. Mederle, R. Borth, C. Geibel, F. M. Grosche, G. Sparn, O. Trovarelli, and F. Steglich: J. Magn. Magn. Mater. **226–230** (2001) 254.
28) M. E. Macovei, M. Nicklas, C. Krellner, C. Geibel, and F. Steglich: J. Phys.: Condens. Matter **20** (2008) 505205.